Journal of Sound and Vibration (2002) **256**(3), 417–431
doi:10.1006/jsvi.2001.4238, available online at http://www.idealibrary.com on IDEAL®

ON THE HORN EFFECT OF A TYRE/ROAD INTERFACE, PART I: EXPERIMENT AND COMPUTATION

R. A. G. Graf, C.-Y. Kuo, A. P. Dowling and W. R. Graham

Engineering Department, University of Cambridge, Trumpington Street, Cambridge CB2 1PZ, England. E-mail: apd1@eng.cam.ac.uk

(*Received* 26 *January* 2001, *and in final form* 3 *December* 2001)

Near the tyre/road contact area, the road surface and the tyre belt form a horn-like geometry, which provides a significant amplification mechanism for sound sources. Measurements have been carried out on a stationary tyre placed on a plane surface in an otherwise anechoic chamber. Following the reciprocal theorem a microphone was placed in the road surface near the contact patch and a white noise source was used in the far field. The amplification by the horn effect can then be determined as a function of frequency for an array of microphone positions relative to the contact patch and the centre of the tyre. These experimental measurements show that the horn effect is responsible for about 10–20 dB increase in noise level. The amplification function shows a distinct interference pattern for higher frequencies and is independent of the longitudinal source position for low frequencies and source positions close to the contact patch. Numerical calculations using the indirect boundary element method have been carried out. These show excellent agreement with the measurements in the frequency regime of the BEM, i.e., up to 2500 Hz. The dependence of the horn effect on primary geometrical parameters such as the effect of the radius of curvature of the shoulders, the load and the width of the tyre has been investigated experimentally and numerically. The broad features of the horn effect are given by the cylindrical geometry of the tyre. The rounded edges of the tyre tend to increase the levels of the minima and shift them to higher frequencies, while slightly decreasing the levels of the maxima. Shape variations due to load can be accounted for by correcting the source distance to the edge of the formed contact patch. The amplification at low frequencies increases with width, the results collapsing onto a single curve as a function of the dimensionless width ω/λ.
© 2002 Elsevier Science Ltd. All rights reserved.

1. INTRODUCTION

Noise generated by highway traffic is responsible for a substantial proportion of environmental noise pollution. Thanks to modern technology, noise from passenger car engines and other mechanical parts has been significantly reduced. As a result, the tyre noise contribution has become more important even at moderate speeds. For passenger cars, the horizontally radiated sound intensity measured at 40 km/h is about 60 dB and increases linearly in the decibel scale up to 80 dB at 120 km/h [1]. This is equivalent to 30 and 90%, respectively, of the overall noise emission from cars and indicates that, above the moderate speed of 50 km/h, the sound generated by the tyres rolling over the road is the dominant noise. Tyre noise from trucks similarly dominates when the speed is higher than 60 km/h [2]. Hence a reduction in tyre/road noise generation will greatly improve the roadside environment and the associated quality of life. To achieve this goal it is essential to understand the mechanisms of noise generation, and thereby facilitate the search for quiet tyre-tread/road surface combinations that do not compromise road safety.

0022-460X/02/$35.00 © 2002 Elsevier Science Ltd. All rights reserved.

For over 30 years this requirement has driven extensive research in both measuring and identifying the tyre noise generation mechanisms, with the aim of reducing the noise at the source. In spite of these efforts, current knowledge still does not enable manufacturers to predict the noise emission of a specific tyre/road combination, and long and expensive tests are necessary for new tyre/road designs. This is due to the number of different mechanisms involved in tyre noise generation and radiation, which often influence each other and which are dependent in a complex way on tyre and road design and operating conditions.

The main sources of sound are deflections of the tyre surface and the resulting air displacements, particularly those associated with tread blocks entering (air pumping) or leaving (tread block snap out) the contact patch (see, for example, reference [3]). These can excite acoustic resonances in the lateral and longitudinal tread grooves leading to large mass flow rates at their ends. All these sources are positioned in the tyre/road gap, where the road surface and the tyre belt form a horn-like geometry. This influences the wave propagation and provides significant amplification, of about 10–20 dB [4–7].

It is thus essential that a tyre/road noise prediction method accounts for the horn effect, and is capable of describing it accurately. The main aim of this paper is to demonstrate this capability, via comparison of experimental measurements with boundary element method calculations. In addition, an improved understanding of the effect follows from the experimental and numerical studies into its dependence on the tyre geometry.

In sections 2 and 3 the horn amplification of sound generated by a simple acoustic source is investigated experimentally. The experimental arrangement exploits the reciprocal theorem which states that the sound pressure level is unchanged when the positions of an acoustic monopole source and listener are interchanged. Thus, the amplification can be determined by locating a microphone in place of a sound source in the tyre/road gap of a stationary tyre in a semi-anechoic chamber and measuring the sound of a distant acoustic source. Due to the small size of the microphone a whole array of source positions in the vicinity of the contact patch can be investigated. The experimental results are compared with the predictions of the boundary element method in section 4. In section 5 an image source model formulated by Ronneberger [4] for the higher frequency range is discussed and compared with experimental results. It is shown that a modified version of this model correctly predicts the horn effect in a wedge made of two intersecting planes, but only quantitatively describes the horn effect of a tyre road gap. An alternative model based on ray theory is proposed for this case and is described in Part 2 of this paper [8]. Finally, the dependence of the horn-effect on different geometrical parameters is investigated both through experiment and boundary element calculations. In section 6 these results and their importance for creating a model to predict the horn effect of a tyre in practical operating conditions are discussed.

2. EXPERIMENTAL ARRANGEMENT

Amplification by the horn-shaped region between the tyre and the road can be determined by placing a known source at different locations in the horn. Provided the source is unaltered by the nearby tyre, its strength can be quantified by measurements without the tyre. However, the horn is a highly confined space and it is hard to place an acoustic source in it without modification by the tyre, e.g., an air jet (monopole without the tyre) may impinge on the tyre leading to an additional dipole. Instead, one can exploit the reciprocal theorem, which states that the measured sound is unaltered when the locations of a fixed monopole source and listener are interchanged. In the reciprocal problem, the source is positioned in the far field and the microphone is placed in the tyre/road gap.

A loudspeaker, capable of generating sound across a wide frequency range, has been found to be a convenient source.

To measure the amplification due to the horn effect, a microphone (B & K, $\frac{1}{4}$ in) is placed in the rigid floor of a semi-anechoic chamber of 7 m $\times$ 4·26 m, with a height of 3·45 m and a cut-off frequency of 200 Hz. The tyre is held by a frame in an upright position above the microphone, as shown in Figure 1. It can be moved in the x direction to vary the distance d between the microphone and the centre of the contact patch and can also be moved in the y direction (axle-direction) to place the microphone at a distance o away from the centreline of the tyre (see Figure 2). The z direction describes the height above the ground of, for example, the loudspeaker. The frame is also used to exert a load on the tyre.

Figure 1 shows the schematic of the experimental arrangement. A loudspeaker with a diameter of 8·5 cm is connected to a white noise generator and positioned in the far field (at $x = 2{\cdot}57$ m and $z = 0{\cdot}72$ m). The signal measured by a 1/4 in microphone in the floor is amplified and an average over 200 samples is taken. The Fourier transform is determined digitally to give the amplitude spectrum of the sound field at the microphone position. The signal is filtered with an anti-aliasing filter with a cut-off frequency of one third of the sampling frequency of $f_s = 30$ kHz. Spectra with and without the tyre present are measured and their ratio yields the amplification as a function of frequency.

Since the tyre is sufficiently far away from the loudspeaker, the sound emitted from the loudspeaker is constant over the area of the tyre. In directivity measurements the loudspeaker is always pointed in the direction of the microphone. Since no absolute measurements are taken, but all measurements are divided by an equivalent one without the tyre being present, any changes in absolute sound levels in different directions of the loudspeaker are of no importance as long as they are constant over the angle the tyre appears. The microphone is small compared to the wavelenght at all frequencies of interest to us. Measurements carried out for the investigation of the directivity, taken without the tyre being present, showed no dependence of the microphone on the angle of incidence of the sound.

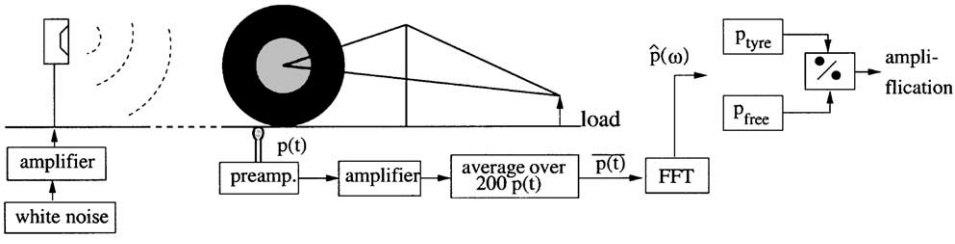

Figure 1. Schematic of the experimental set-up. Spectra with and without the tyre present are measured and their ratio yields the amplification as a function of frequency.

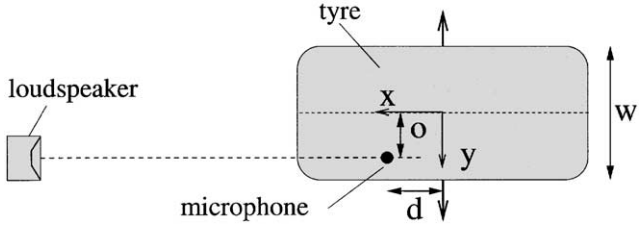

Figure 2. Definition of the co-ordinate system and variables: the width of the tyre w, the distance between axle and microphone d and the distance from the microphone to the centreline of the tyre o.

3. THE HORN EFFECT OF A SOLID SIMPLIFIED CYLINDER

As a first, simplified, experiment the complex geometry of a tyre is replaced by a solid cylindrical drum (diameter, 64 cm; width, 20 cm) consisting of a smooth steel belt with flat wooden side walls. In Figure 3 the amplification by the horn effect is shown. The microphone was placed on the centreline of the cylinder and the distance d between microphone and axle was varied. The results show that the horn effect can be significant, with amplification in excess of 20 dB for some frequencies and small d. As most of the sources for tyre/road generated noise are expected to be found close to the contact patch, i.e., at small d [9], this is the most relevant situation.

Three characteristic features can be noted. First the amplification tends to 0 dB as the frequency goes to zero. This can be explained by the fact that the diameter of the cylinder becomes small compared to the wavelength of the acoustic wave as $f \to 0$. The cylinder is then acoustically invisible and therefore no amplification is observed.

At higher frequencies an interference pattern with distinct minima can be seen. The frequencies at which the minima occur depend strongly on the distance d. This is due to destructive interference and can be explained by image sources [4] or ray theory [10].

At low frequencies the amplification is independent of d up to a maximum frequency which depends on d (Figure 4). If d is sufficiently small ($d \leqslant 30$ mm), the amplification is

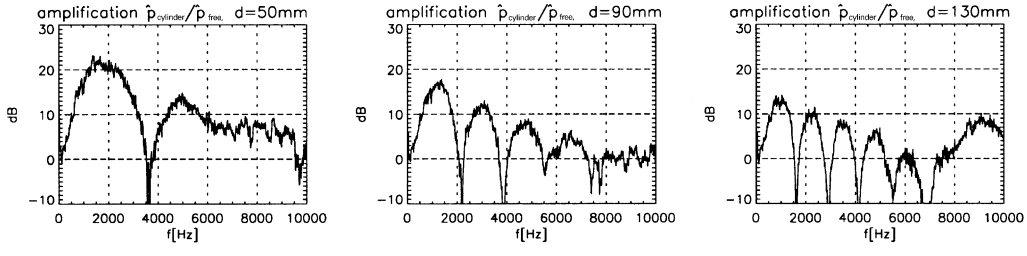

Figure 3. Amplification by the horn effect of a solid cylinder as a function of frequency for different distances d between microphone and axle.

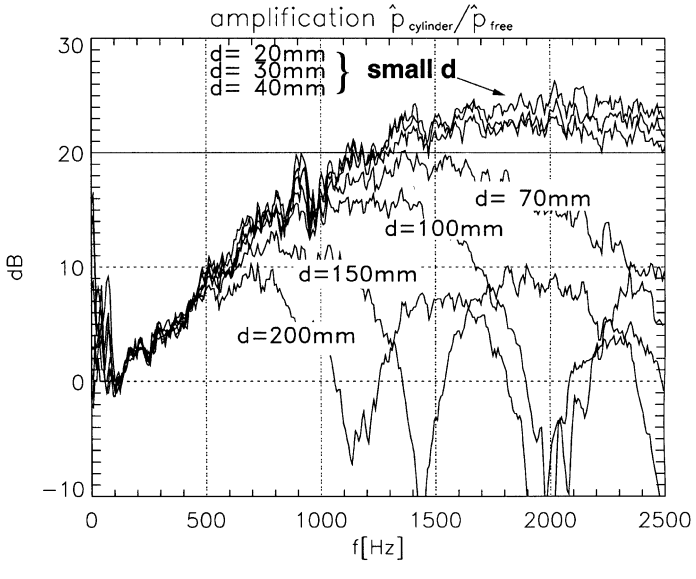

Figure 4. Dependence of the amplification on d.

virtually independent of d up to about 2 kHz. Since this is the frequency range where tyre noise is most dominant the modelling of the horn effect is greatly simplified. Exact information about the source position is not needed as long as the source is close to the contact patch.

4. NUMERICAL CALCULATIONS

The boundary element method is widely used for three-dimensional problems involving acoustic wave propagation in a stationary medium [11]. This method is particularly advantageous in external sound field calculations because the infinite physical domain does not need to be discretized and the outgoing wave boundary condition at infinity is automatically satisfied.

The aim of the numerical investigation is to validate the experimental results and to find the primary geometrical parameters influencing the sound propagation. Both tyre and road surface are assumed to be rigid.

Calculations were carried out by using Comet Version 4·0 on an SGI O2 workstation [12]. Here again the reciprocal theorem is exploited, significantly reducing the amount of calculation time needed to investigate the dependence of farfield sound on the nearfield source location for a fixed farfield listener. For a monopole sound source at a fixed position in the far field the sound pressure distribution on a data recovery mesh is calculated near the contact patch of a solid cylindrical drum of the same dimensions as the one used in the acoustical measurements. This data is then divided by the sound pressure obtained when the drum is not present in order to yield the amplification function. Since a mesh density of at least four to five nodes per wavelength is required the BEM calculation is limited by the computer storage capacity to a frequency range of upto 2·5 kHz. Approximately 1500 nodes were used in the calculations.

Both direct and indirect boundary element methods were used in the calculations. There are basically two differences between the two methods. Firstly in the direct method the Helmholtz integral equation is used, treating the interior and exterior domain separately, with the primary variables being the pressure and velocity on the surface. In the indirect method, which can be treated as a special case of the direct method, a combination of the Helmholtz integral equations for the interior and exterior domain is used, and both domains are computed simultaneously. The primary variables are the differences in the pressure and in the gradient of pressure between the inside and outside of the surface (giving a source density function on the surface). In the direct method the system of equations required to calculate the sound field relates to an asymmetric matrix, whereas the indirect method uses a variational formulation to compute the sound field radiated, which results in assembling a symmetric system of equations, therefore saving memory space and calculation time.

Since the indirect method was found to be more robust only the results from this approach are shown in the following. Figure 5 shows the boundary mesh of the cylinder and the data recovery mesh for the BEM calculation. A typical distribution of the sound amplification on the data recovery mesh is shown for a source frequency of 1100 Hz. The interference pattern can be clearly seen near the centreline of the tyre. The pressure level decreases to the sides of the tyre. The calculation for small values of d was problematic and it was found to be improved by reducing the size of the mesh elements in the contact patch region. For the shown mesh the numerical calculations were possible for values of d of 3 cm and more. A careful remeshing in the contact patch vicinity might improve this further. Fortunately however it was found, as mentioned above, that the results are independent of d at these small values of d in the frequency range of interest, so that these numerical

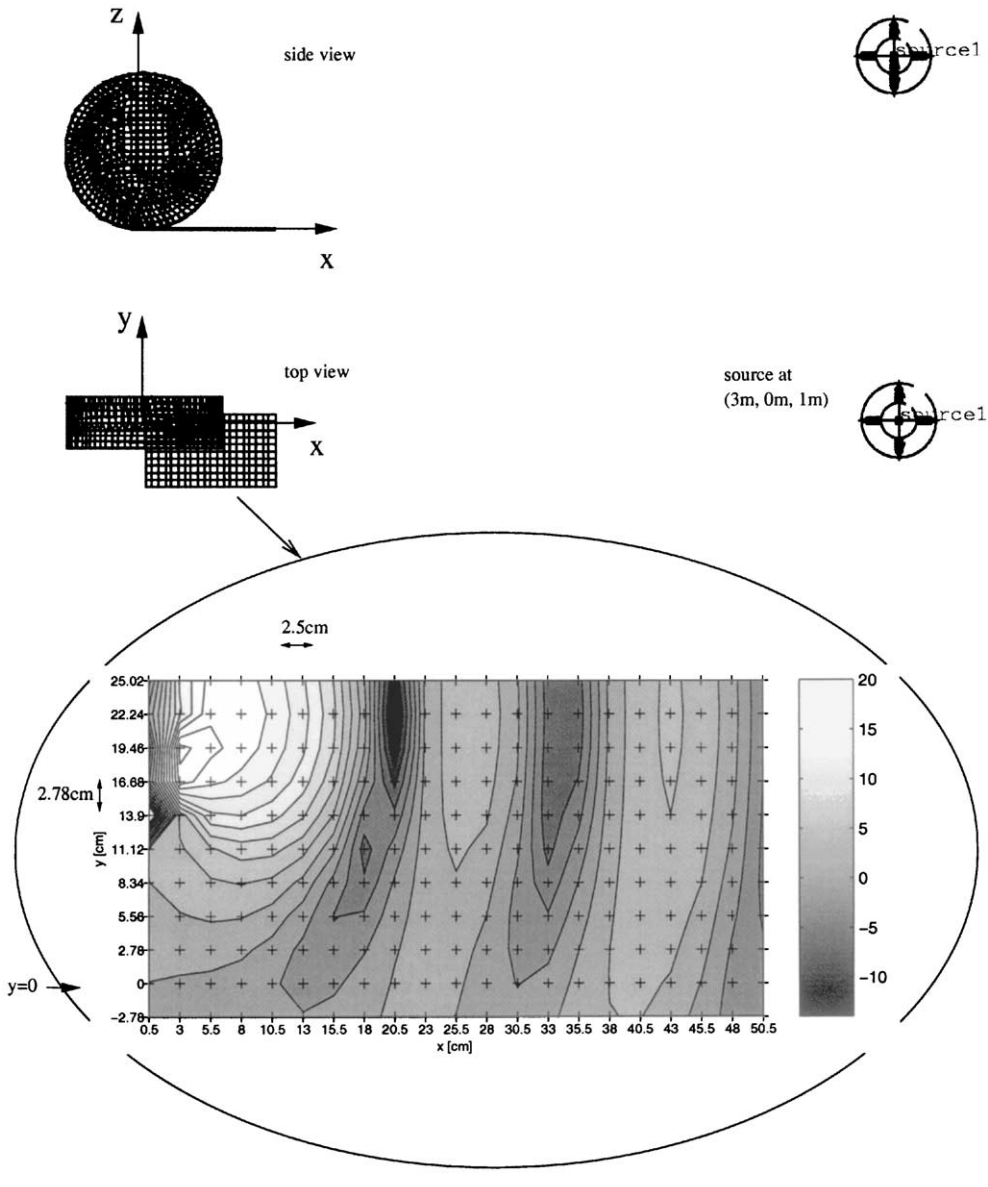

Figure 5. Top: Data recovery mesh for the BEM calculation, showing the source at (3, 1, 0) m, the boundary mesh of the cylinder shape and the data recovery mesh on the perfectly rigid half plane. Bottom: Distribution of sound amplification on data recovery mesh for source frequency 1100 Hz.

difficulties do not pose a problem. In Figure 6 the BEM calculations are compared with experimental results for the three nearest values of d. The comparison shows excellent agreement, thus validating the BEM implementation presented here.

Similar calculations have recently been carried out [6].

5. HIGH FREQUENCY MODELS

A model for interference pattern of the horn effect at higher frequencies has been proposed by Ronneberger [4], who simplified the tyre/road gap to a semi-infinite wedge.

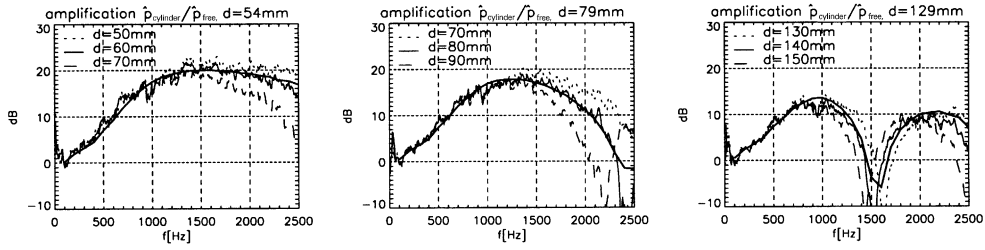

Figure 6. BEM calculation for the solid cylinder (——) compared with experimental results for the three nearest values of d.

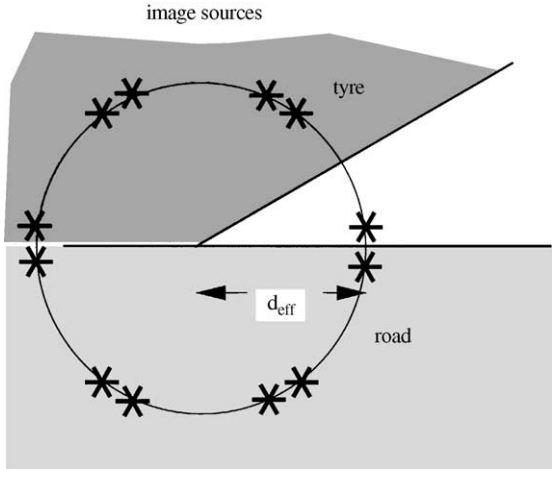

Figure 7. Location of image sources for a semi-infinite wedge.

The boundary conditions can be described by multiple image sources (Figure 7). In Ronneberger's model the total source strength is then evenly distributed over the circle on which the image sources lie, yielding an analytical function describing the amplification as a function only of the wedge angle α and the distance d between the source and the contact line. The comparison with the measurements for a cylinder in Figure 8 shows that the general shape of the amplification function is reproduced, but Ronneberger's model does not fully resolve the correct lobe structure.

The reason is his neglect of the curvature of the tyre, which changes the boundary condition, resulting in a different interference pattern. In order to show this, Ronneberger's model is compared in Figure 9 with measurements carried out with plane wooden boards placed at an angle α to the floor. The lobe structure is predicted correctly for the smaller angle, $\alpha = 10^\circ$. For the larger angle, $\alpha = 20^\circ$, Ronneberger's smearing of the source strength over the circle is no longer a legitimate approximation since the distance between two image sources is no longer small compared to the wavelength in the frequency range of interest. In this case, it is preferable to sum the contributions from the image sources numerically. This *image source model* is also shown in Figure 9. At lower frequencies it coincides with Ronneberger's analytical expression, but at higher frequencies (above 7·5 and 3 kHz for $\alpha = 10$ and 20°, respectively) it differs, reproducing the experimental results with much greater fidelity.

The image source model is limited, in that it works only for integer values of $2\pi/\alpha$. A ray theory which is capable of describing the amplification by the wedge for all possible angles

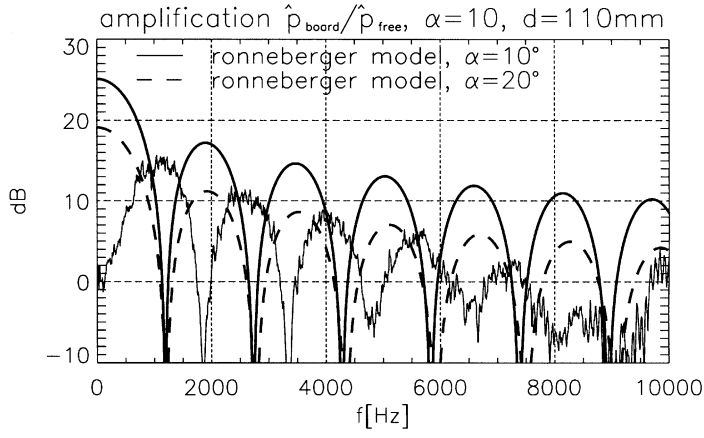

Figure 8. Comparison of Ronneberger's model for two angles α with measurements of the amplification by a cylinder.

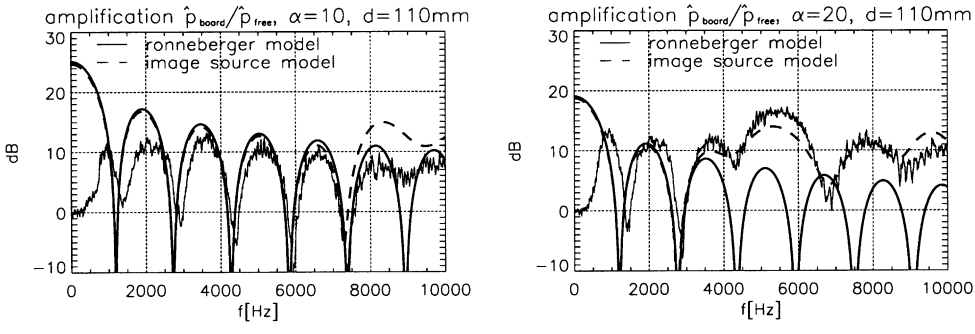

Figure 9. Comparison of Ronneberger's model and the ray theory wedge model with measurements of the amplification by plane wooden boards placed at two different angles α to the floor.

α has been developed by Kuo [10]. This theory can also be extended to include the curvature of the cylinder and can therefore predict the horn effect of a real tyre at higher frequencies. This work is discussed in the second part of this paper [8].

6. DEPENDENCE ON GEOMETRY

Under real traffic conditions the scatterers are real tyres loaded by the weight of the car. To investigate the influence of the tyre shape on the amplification characteristics a smooth tyre (without any tread pattern) pressured to 1·7 bar gauge has been tested under loads of 0 and 250 kg. The tyre is a Dunlop SP 3000, of diameter 63·5 cm and width 20 cm. The shape of the tyre with and without load is shown in Figure 10. The results of measurements of the horn amplification by an unloaded tyre are very similar to those of the cylinder (Figure 11).

For the cylinder the amplification for low frequencies is slightly higher, the dips are more distinct and the minima are at lower frequencies. This was surmised to be an effect of the rounded shoulders of the tyre, the most obvious departure from the cylindrical geometry. To investigate this further, calculations with the BEM were carried out. The corner effect is expressed in terms of the radius of curvature of the round edges. Three radii (0, 30 and

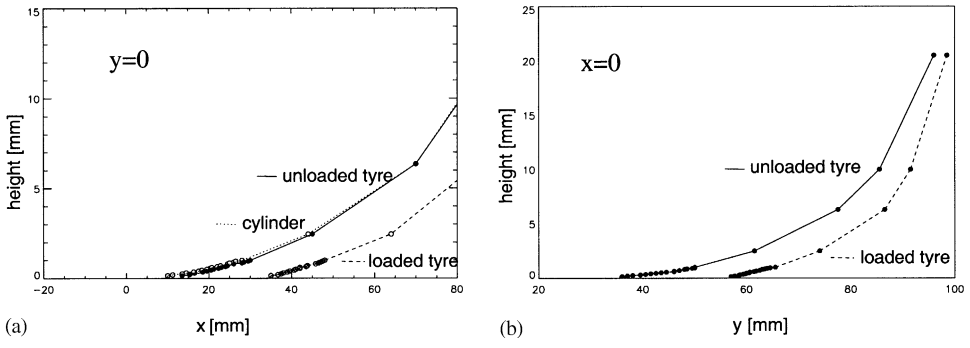

Figure 10. (a) Shape of the cylinder, unloaded and loaded tyre for the centreline ($y = 0$) as a function of x, (b) unloaded and loaded tyre at the axle position ($x = 0$) as a function of y.

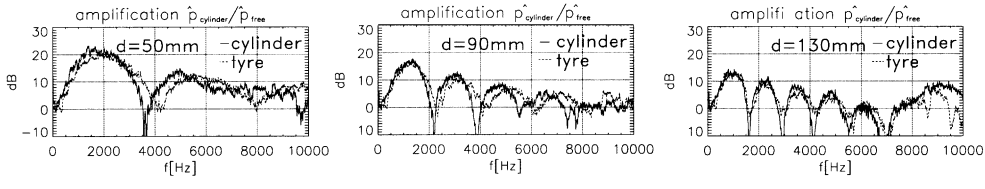

Figure 11. Comparison of the amplification by a cylinder and an unloaded tyre $d = 50$, 90 and 130 mm.

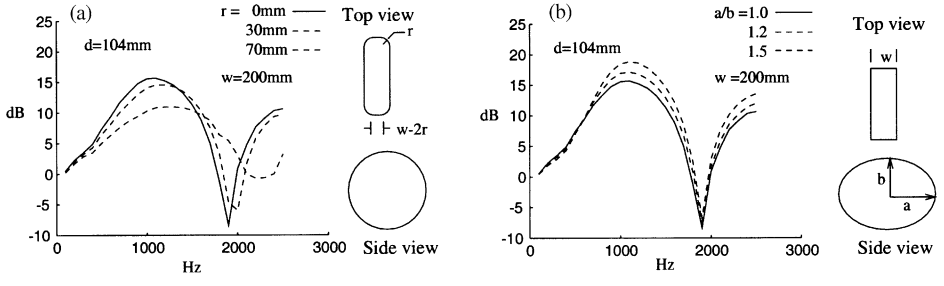

Figure 12. (a) Amplification by a solid cylinder with rounded edges of different radii, (b) amplification by an elliptic solid cylinder for different aspect ratios.

70 mm) with a fixed side-to-side width of 20 cm have been investigated (Figure 12(a)). The results show that the smooth corner smears the dip of the acoustic interferences, reduces the maximum amplification, and shifts the minima to higher frequencies, in agreement with the experimental results in Figure 11.

The cylinder and tyre geometries also differ in the nature of their contact with the ground plane. The tyre, loaded either by its own weight or by the extra load of the car, has a finite contact patch. The effective distance d_{eff} between the microphone and the *edge* of the contact patch, which determines the interference pattern of the amplification-function, is therefore shorter for the unloaded tyre and even shorter for the loaded tyre for the same distance d between the microphone and the *centre* of the contact patch.

A load of 250 kg on the tyre elongates the contact patch by 4 cm (Figure 10(a)). The overall shape of the tyre also changes with its load. Again using the BEM, the influence of the tyre shape can be investigated. It can be simulated by elliptical side-walled cylinders with long and short axes a, b (Figure 12(b)). The interference pattern minima remain at the

same position with varying aspect ratio but the maximum amplification increases by about 5 dB around 1000 Hz for the largest aspect ratio considered, $a/b = 1{\cdot}5$.

However, from a comparison of the curves for a tyre with and without load for the same d_{eff} in Figure 13 it can be seen that the curves differ very little. The minima are deeper for the loaded tyre which agrees with the tendency the BEM-calculation shows for a cylinder with sharper edges. The radius of curvature near the contact patch reduces with load, since the contact patch widens, so that the horn effect of a loaded tyre appears to be closer to that for a tyre with sharper edges. However, the amplitude of the amplification found in the experimental measurements does not change with the load: although the computations in Figure 12(b) predict an increase due to both the sharper edges and the higher aspect ratio of the loaded tyre, these trends are only significant for extreme distortions. In practice, the minor change in shape due to a load of 250 kg has a negligible effect on the total amplification. This has been found to be true even for more severe deformations occurring for a tyre pressured to 0·7 bar gauge and the same load of 250 kg, which corresponds to a deformation a tyre experiences in real road conditions. The effect of load can therefore be solely characterized by the shape of the contact patch, which greatly simplifies the modelling of the horn effect of tyres under real traffic condition.

Finally, width effects have been investigated using the wedge geometry introduced in section 5. Boards of three different widths ($w = 20$, 26 and 40 cm) were tested, and the results are presented in Figure 14. The main influence of width can be seen to be at low frequencies. It has already been noted that for the lowest frequencies the amplification for cylinder and tyre is independent of the distance d between the centre of the contact patch and the microphone (Figure 4). The amplification by the plane boards is again independent of d for

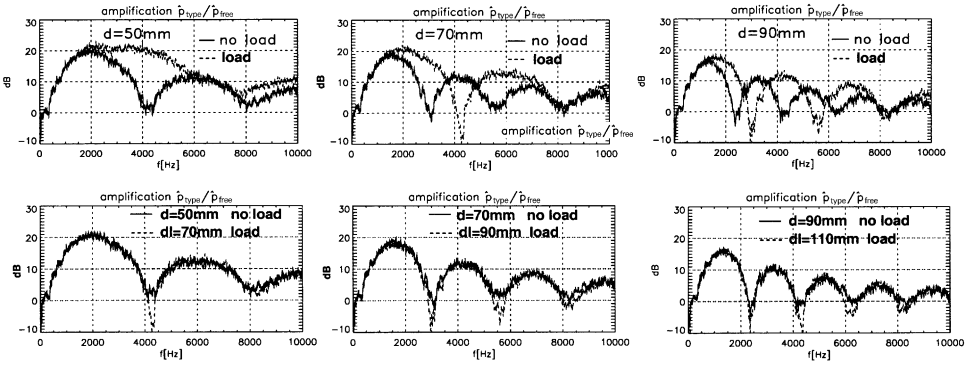

Figure 13. Amplification for a tyre for d without load (——) and $dl = d + 20$ mm with load (·····), and therefore the same d_{eff}.

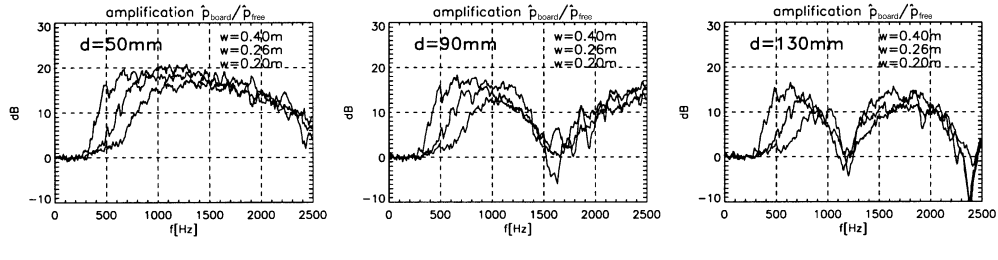

Figure 14. Amplification by a plane wooden board with $\alpha = 10°$ for different distances d between microphone and contact line. The different graphs compare different board widths w: $w = 0{\cdot}20$ m, 0·26 m and 0·40 m, where the highest amplification at low frequencies is connected with the widest board.

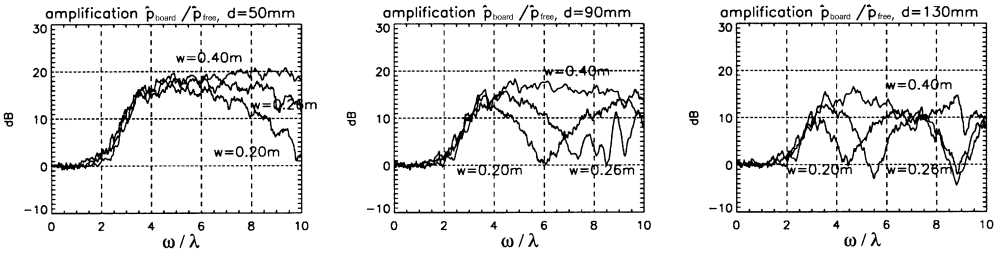

Figure 15. Amplification by boards of different widths w as a function of the ratio ω/λ. Different graphs show different d.

the low frequencies but is a function of the board width so that the widest board has the highest amplification at a given frequency (Figure 14). In fact, the amplification is dependent only on the ratio between wavelength and width w (Figure 15), and not on each parameter alone. This can be explained by a simplified low frequency asymptotic theory, which is presented in the second part of this paper [8].

7. OFFSET MEASUREMENTS

Up to now only the amplification of sound generated at the centre of the tyre has been discussed. However to understand the amplification of sound generated by a rolling tyre all possible positions of the sound sources have to be considered. Air pumping, tread block snap out and longitudinal grooves will generate sound over the whole width of the tyre tread in front of and behind the contact patch. Lateral groove resonances will also lead to sound from the sides of the contact patch.

Measurements have been carried out by moving the cylinder or tyre along its axle. By doing so the microphone in the floor becomes positioned a distance o away from the centreline of the tyre (see Figure 2) with source and listener remaining in the same position relative to each other. The effect of this offset on the amplification by the cylinder, the unloaded tyre and the loaded tyre has been investigated.

Figure 16 shows the amplification of a solid cylinder with sharp edges for different offsets o. The amplification decreases with o. Although the sound amplification at the edge of the tyre is considerably less than at the centre of the tyre, it is by no means negligible. For example for the cylinder at $d = 5$ cm, the maximum amplification drops from 22 dB for $o = 0$ to about 8 dB for $o = 10$ cm. These results can be accurately reproduced by BEM calculations, which are also shown in Figure 16. The amplification by loaded and unloaded tyres shows the same tendency. However, due to the curved shape of the contact patch, the longitudinal distance between the microphone and the edge of the contact patch d_{eff} is a function of the offset o. Detailed information on the shape of the contact patch (which varies with load) is needed to determine the appropriate d_{eff}, but once it is known a good collapse between results for the loaded and unloaded tyres has been found.

8. DIRECTIVITY

Knowledge of the directivity of the horn effect is essential to predict tyre/road noise sound levels as a vehicle passes by.

The horn effect directivity was investigated experimentally and numerically. Measurements were carried out as described in section 2. The loudspeaker was moved to

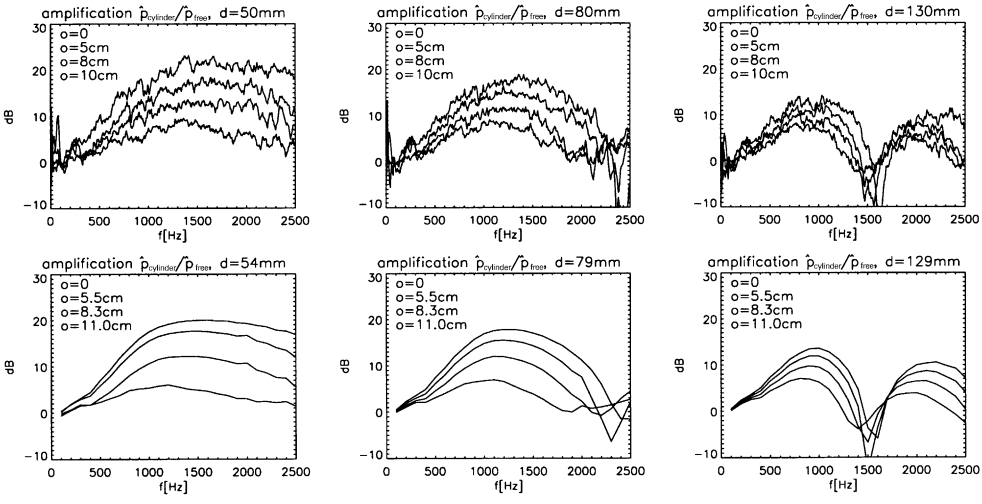

Figure 16. Amplification by the cylinder for different offsets *o*. Different graphs show different values of *d*. Top: measurements, bottom: BEM calculation.

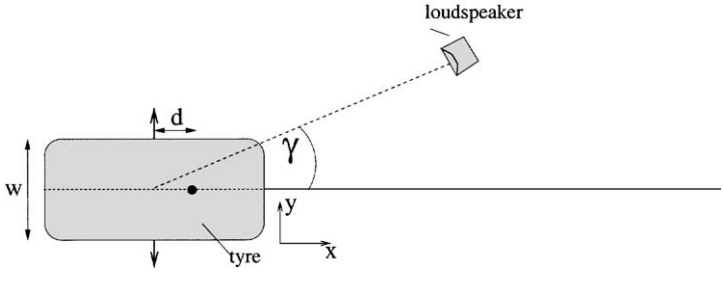

Figure 17. The angle between the forward direction and the direction of the loudspeaker is denoted as γ.

different locations around a circle of radius of 1·80 m, centred on the tyre axle at a height of 0·08 m above the floor. The angle between the tyre centreline and the direction of the loudspeaker is denoted as γ (Figure 17). Results are shown for angles $-90^\circ < \gamma < 90^\circ$. Measurements at higher angles of γ were contaminated by scattering from the frame holding the tyre and results for $|\gamma| > 90^\circ$ are therefore not shown in the following. This scattering as well the white noise nature of the sound source causes a scattering of the amplification function of about ± 2 dB. In order to determine the amplification value at a certain frequency *f*, a sample of 41 points was taken from the discretised amplification function, representing a frequency interval of 300 Hz centered around *f*. The value of the amplification function at *f* was found by linear regression of the 41 values. The error is given as 1·5 times the standard deviation of the distance between the data points and the linear fit in that frequency interval. This approximation of the experimental data was found to be a reasonable estimation of the correct amplification, with the main problem of slightly overestimating the values in the frequency dips.

In addition to the experimental investigation numerical calculations were carried out using the boundary element method described in section 4.

In Figures 18 and 19 the experimental and numerical results are compared for six different frequencies. Figure 18 shows the experimental results for the cylindrical drum

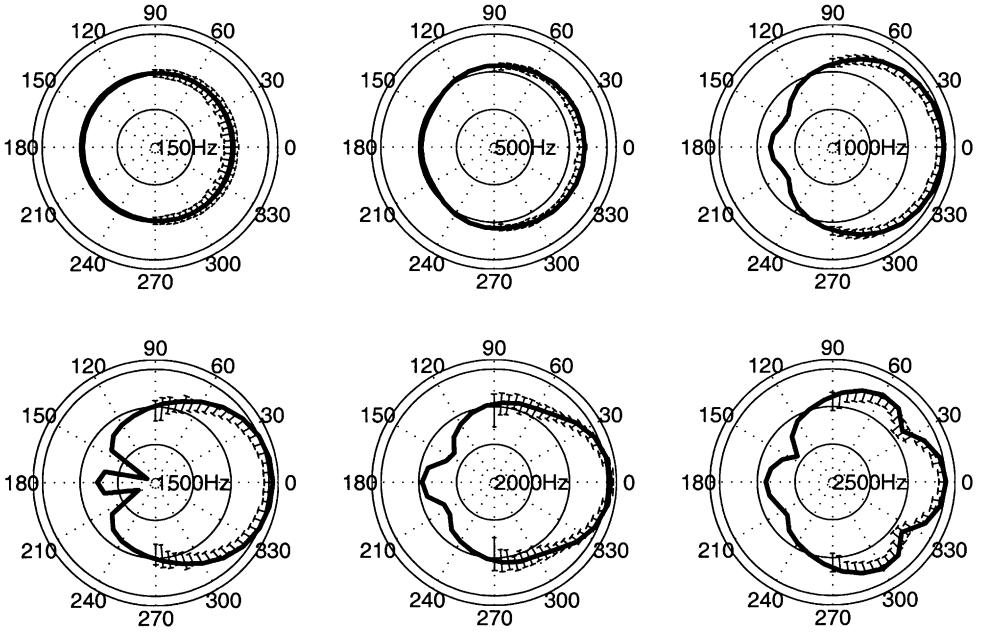

Figure 18. BEM calculation for the solid cylinder with sharp edges (thick solid line) compared with experimental results for a cylindrical drum. The circles indicate sound levels of − 40, − 20, 0, 20 and 25 dB.

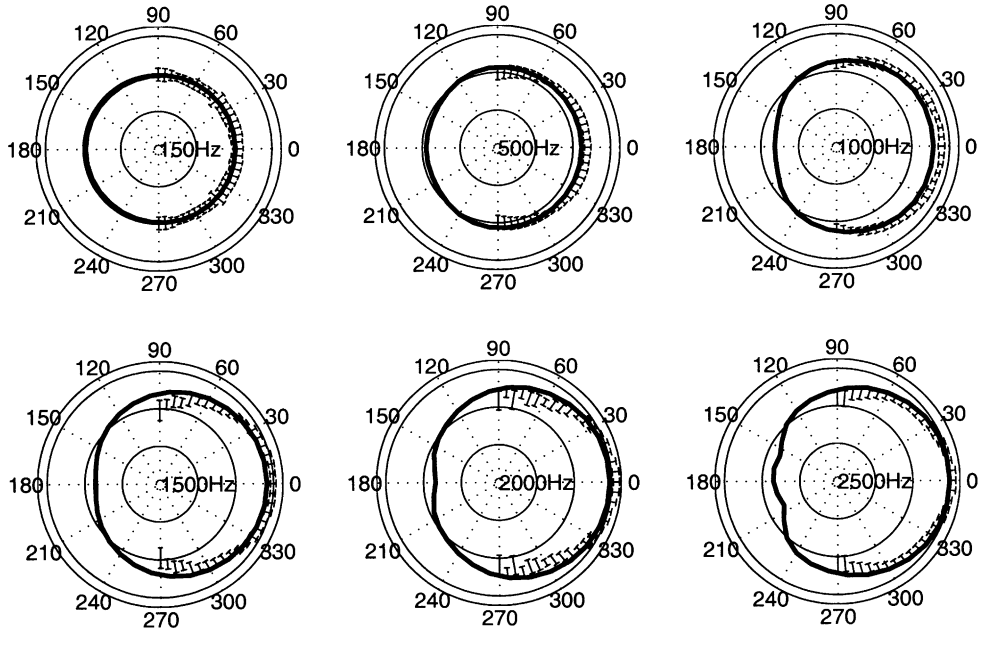

Figure 19. BEM calculation for the solid cylinder with an edge radius of 7 cm (thick solid line) compared with experimental results for a loaded tyre. The circles indicate sound levels of − 40, − 20, 0, 20 and 25 dB.

(described in section 3) and BEM calculations for a cylindrical drum with sharp edges. Figure 19 shows the experimental results for the tyre loaded with 250 kg and BEM calculations for a cylindrical drum with an edge radius of 7 cm chosen to match the shape of

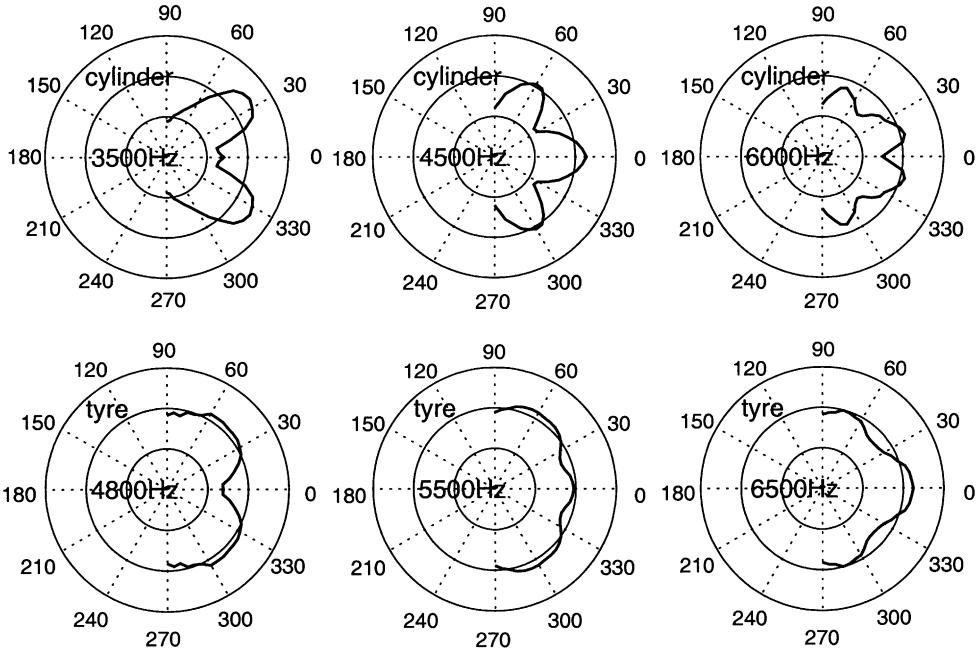

Figure 20. Experimental results for cylinder (top) and tyre (bottom) for higher frequencies. The solid line circles indicate sound levels of -10, 0, 10 and 20 dB.

the loaded tyre in the contact patch region. The comparison shows excellent agreement in both cases, even resolving the effects of the shoulder radius, and therefore proving the BEM to be capable of accurately predicting the horn effect directivity.

The cylinder case shows a distinctive lobe structure which is less pronounced in the tyre case. The number of lobes increases with frequency and for higher frequencies it is also present for the tyre case (Figure 20). At $\gamma = 45^\circ$ an amplification of up to 15 dB can be found for both the tyre and the cylinder case, reducing to -3 to 5 dB amplification at $\gamma = 90^\circ$. It is interesting to note that the maximum amplification is not always on the centreline of the tyre (Figure 20).

9. CONCLUSIONS

The horn effect, whereby noise generated at the tyre/road interface is amplified and transmitted to the far field, has been investigated experimentally and numerically. A maximum amplification of around 22 dB at 2 kHz has been found for a representative car tyre geometry. For low frequencies and small d the amplification is independent of the longitudinal distance between source and contact patch d and approaches zero dB at $f \to 0$. The amplification increases with width w, but the curves collapse onto a single function of the dimensionless frequency ω/λ.

For the frequency range ($f < 2500$ Hz) the BEM provides an effective tool to calculate the horn effect for practical geometries giving predictions that are in excellent agreement with experiment. However, this numerical solution does not give a physical explanation for the striking frequency dependence of the horn amplification. In Part II, high and low frequency asymptotic theories are developed which clearly highlight the mechanisms

influencing the character of the amplification. Comparison is made between a tyre and a cylinder of the same diameter and width, but with a sharp edge.

At high frequencies ($f > 2500$ Hz), an interference pattern dominates the amplification function. The broad features of the high frequency interference pattern are similar, although there are some differences in the details. In particular, the rounded edges of the tyre tend to increase the levels of the minima and shift them to higher frequencies, while slightly decreasing the levels of the maxima. Shape variations due to load can be accounted for by correcting the source distance to account for the shift in the origin of the horn geometry due to the formation of a contact patch. Thus, loaded tyres in real traffic situations can be modelled by the unloaded tyre as long as the different shape of the contact patch is taken into account. As the source location moves across the belt towards the edge of the tyre, the amplification decreases, but an amplification of up to 8 dB has still been found at the edge. This is considerably less than at the centre (up to 22 dB), but by no means negligible.

The directivity of the horn effect was investigated experimentally and numerically for the cylinder and tyre case. The agreement is excellent in both cases, even resolving the effect of the shoulder radius. The maximum amplification has been shown not to be always on the centreline of the tyre, due to a distinctive lobe structure which is less pronounced for the tyre case. The ability to predict the horn effect demonstrated here is thus central to achieving an accurate model of tyre/road noise.

ACKNOWLEDGMENTS

This research has been made possible with the support of a "DAAD Doktorandenstipendium im Rahmen des gemeinsamen Hochschulsonderprogramms III von Bund und Ländern" and the EPSRC under the Inland Surface Transport Link Programme. It has been carried out in collaboration with Dunlop Tyres Ltd., the TRL and the Landrover Group, UK, whose contributions and interest are gratefully acknowledged.

REFERENCES

1. D. Ronneberger 1989 *Physik in unserer Zeit*, 20. *Jahrg*., *Mai* 1989, Vol. 3, 81. Verkehrslärm: Rollgeräusche.
2. W. Kropp 1989 *Applied Acoustics* **26**, 181. Structure-borne sound on a smooth tyre.
3. M. Heckl 1986 *Wear* **13**, 157–170. Tyre noise generation.
4. D. Ronneberger 1982 *INTER NOISE*, *May* 1982, *San Francisco*, *USA*, 131. Noise generation from rolling tires—sound amplification by the "horn effect".
5. D. Ronneberger 1989 *Workshop on rolling noise generation*, *Institut fur Technische Akustik Technische Universität*, *Berlin*. Towards quantitative prediction of tyre/road noise.
6. W. Kropp, F.-X. Becot and S. Barrelet 2000 *Acta Acoustica* **86**, 769–779. On the sound radiation from tyres.
7. R. A. G. Graf, C. Y. Kuo, A. P. Dowling and W. R. Graham 1999 *Proceedings INTERNOISE Conference* 1999, *Ft. Lauderdale*. Horn amplification at a tyre/road interface—Part I: experiment and computation.
8. C. Y. Kuo, R. A. G. Graf, A. P. Dowling and W. R. Graham 2002 *Journal of Sound and Vibration* **256**, 433–445. On the horn effect of a tyre/road interface—Part II: asymptotic theories (submitted).
9. K. Iwao and I. Yamazaki 1996 *JSAE Review* **17**, 139–144. A study on the mechanism of tyre/road noise.
10. C. Y. Kuo, R. A. G. Graf, A. P. Dowling and W. R. Graham 1999 *Proceedings INTERNOISE Conference* 1999, *Ft. Louderdale*. Horn amplification at the tyre/road interface—Part II: ray theory and experiment.
11. R. D. Ciskowski and C. A. Brebbia ed. 1991 *Elsevier Applied Science*. Boundary element methods in acoustics.
12. COMET acoustics software, developed by Automated Analysis LTD, now owned by Collins & Aikman see http://www.colaik.com/prod/acoustics/sw.html